Biochimica et Biophysica Acta 1840 (2014) 1651–1656

Contents lists available at ScienceDirect

Biochimica et Biophysica Acta

journal homepage: www.elsevier.com/locate/bbagen

Comparison of quantum dot-binding protein tags: Affinity determination by ultracentrifugation and FRET

Mara Werwie [a], Niklas Fehr [a], Xiangxing Xu [b,1], Thomas Basché [b], Harald Paulsen [a,*]

[a] Institut für Allgemeine Botanik, Johannes-Gutenberg-Universität Mainz, Johannes-von-Müllerweg 6, 55099 Mainz, Germany
[b] Institut für Physikalische Chemie, Johannes-Gutenberg-Universität Mainz, Duesbergweg 10-14, 55128 Mainz, Germany

ARTICLE INFO

Article history:
Received 16 July 2013
Received in revised form 7 November 2013
Accepted 25 November 2013
Available online 19 December 2013

Keywords:
Nanoparticle
Protein
Stoichiometry
Ultracentrifugation
Fluorescence resonance energy transfer (FRET)
Light-harvesting complex II (LHCII)

ABSTRACT

Background: Hybrid complexes of proteins and colloidal semiconductor nanocrystals (quantum dots, QDs) are of increasing interest in various fields of biochemistry and biomedicine, for instance for biolabeling or drug transport. The usefulness of protein–QD complexes for such applications is dependent on the binding specificity and strength of the components. Often the binding properties of these components are difficult and time consuming to assess.
Methods: In this work we characterized the interaction between recombinant light harvesting chlorophyll *a*/*b* complex (LHCII) and CdTe/CdSe/ZnS QDs by using ultracentrifugation and fluorescence resonance energy transfer (FRET) assay experiments. Ultracentrifugation was employed as a fast method to compare the binding strength between different protein tags and the QDs. Furthermore the LHCII:QD stoichiometry was determined by separating the protein–QD hybrid complexes from unbound LHCII via ultracentrifugation through a sucrose cushion.
Results: One trimeric LHCII was found to be bound per QD. Binding constants were evaluated by FRET assays of protein derivatives carrying different affinity tags. A new tetra-cysteine motif interacted more strongly ($K_a = 4.9 \pm 1.9\ nM^{-1}$) with the nanoparticles as compared to a hexahistidine tag (His_6 tag) ($K_a \sim 1\ nM^{-1}$).
Conclusion: Relative binding affinities and binding stoichiometries of hybrid complexes from LHCII and quantum dots were identified via fast ultracentrifugation, and binding constants were determined via FRET assays.
General significance: The combination of rapid centrifugation and fluorescence-based titration will be useful to assess the binding strength between different types of nanoparticles and a broad range of proteins.

1. Introduction

Colloidal semiconductor nanocrystals or quantum dots (QDs) are widely used for labeling biological components [1–3]. The advantages of QDs compared to fluorescent dyes include their high photostability and their tunable, size dependent absorption and fluorescence emission bands. Their strong fluorescence makes them excellent candidates for fluorescence resonance energy transfer (FRET) studies for example with fluorescent-dye labeled biomaterials [4–6]. As a further advantage, QD–protein (or peptide) conjugates often form spontaneously and several strategies have been described for this self-assembly. Poly histidine tags chelate metal ions on the surface of ZnS-coated core/shell QDs [7–11]. A strong affinity to ZnS surfaces was also observed with peptides containing multiple repeats of cysteine pairs [12]. Furthermore, electrostatic interactions between charged ligands on QD surfaces and protein domains [13,14] or membrane surfaces [15] carrying the opposite charges have been employed for complex formation.

If QDs are to be applied as protein labels, it is helpful to know the QD–protein stoichiometry or to establish strategies to make hybrid complexes at defined ratios. Hybrid complexes of QDs and polyhistidine-tagged proteins at different stoichiometries were separated by gel electrophoresis [10]. This method has also been used in combination with Western blotting, to approximate the average stoichiometries of antibody conjugated QDs [16]. The protein–QD stoichiometry in hybrid complexes has been (roughly) estimated by analytical ultracentrifugation [17]. In another approach the formation of protein–QD assemblies at a 1:1 ratio was revealed by atomic force microscopy [18]. All methods have in common that they are rather complex and/or can give only a rough estimate of the QD–protein stoichiometry.

Here we present a very simple and fast method to assess different protein affinity tags with regard to their efficiency in promoting QD–protein binding and to average QD–protein stoichiometries. By using rapid ultracentrifugation, QD–protein complexes were separated from unbound protein. FRET assays were used to estimate the binding constants of different binding tags.

In the experiments described here, type-II CdTe/CdSe/ZnS QDs were used that were functionalized with dihydrolipoic acid (DHLA) for water-solubility. The protein component to be bound to QDs was recombinant light harvesting complex II (LHCII), reconstituted in vitro

* Corresponding author.
E-mail address: paulsen@uni-mainz.de (H. Paulsen).
[1] Present address: State Key Laboratory of Coordination Chemistry, School of Chemistry and Chemical Engineering, Nanjing University, Hankou Road 22, Nanjing, CN 210093, People's Republic of China.

0304-4165/$ – see front matter © 2013 Elsevier B.V. All rights reserved.
http://dx.doi.org/10.1016/j.bbagen.2013.11.025

from its bacterially expressed apoprotein and plant pigments (14 chlorophyll and 4 carotenoid molecules per protein) [19]. The recombinant nature of the protein opens up the possibility of introducing different affinity tags for comparison, without altering the protein structure otherwise. The chlorophylls bound to LHCII are endogenous fluorophores that can be used to monitor protein binding to QDs by serving as acceptors of the QD excitation energy [14].

2. Experimental section

2.1. LHCII variants

Recombinant LHCII was reconstituted from a bacterially expressed protein and plant pigments. Wild type (wt) Lhcb1*2 (AB80) from *Pisum sativum* [20] and its derivatives were used, one with an additional hexahistidyl (His_6) tag at the C-terminus (wt-h) [21] and another one lacking 11 amino acids at the N-terminus (ΔN11) [22]. The derivatives ΔN11-h [23] and h-ΔN11 exhibit the same amino acid sequence as ΔN11 but contain a C-terminal and an N-terminal His_6 tag, respectively, whereas the LHCII derivative h-ΔN11-h contains both an N- and a C-terminal His_6 tag. The plasmids coding for h-ΔN11 and for h-ΔN11-h were constructed by PCR using the plasmids coding for ΔN11 and ΔN11-h, respectively, and primers introducing an N-terminal His_6 tag. The derivative Z8-ΔN11 consists of the same amino acid sequence as ΔN11 but contains, at its N terminus, a ZnS specific binding tag called Z8 [24]. The LHCII variant 4-Cys consists of the same amino acid sequence as the wild type LHCII except of a tetra-cysteine motif (Cys-Cys-Pro-Gly-Cys-Cys) between amino acids 8 and 9. Both the Z8 and the 4-Cys were produced as described for h-ΔN11 and h-ΔN11-h. A scheme of the used LHCII variants is presented in Fig. 1.

2.2. Preparation of recombinant LHCII trimers

The proteins were expressed in *Escherichia coli* as described earlier [22]. Total pigment extract, chlorophylls *a* and *b*, and carotenoids were isolated from pea thylakoids [25]. LHCII apoproteins were reconstituted with pigments to form monomeric LHCII by the detergent exchange method [19], and trimerization was carried out by affinity chromatography for His_6 tag-containing LHCII versions [26] or by trimerization in liposomes according to [23] for LHCII versions without His_6 tag.

For separating monomers and trimers and for removing unbound pigments and unfolded protein, the reconstituted complexes were ultracentrifuged through a sucrose density gradient as described earlier [27] but with a modified buffer (50 mM sodium-phosphate, pH 8.5, 0.1% (w/v) dodecyl-maltoside, 0.6 M sucrose). The trimer band was extracted from the sucrose gradient after centrifugation and its spectroscopic properties were checked by absorption, fluorescence, and CD measurements [22]. The recombinant LHCII complexes contained per

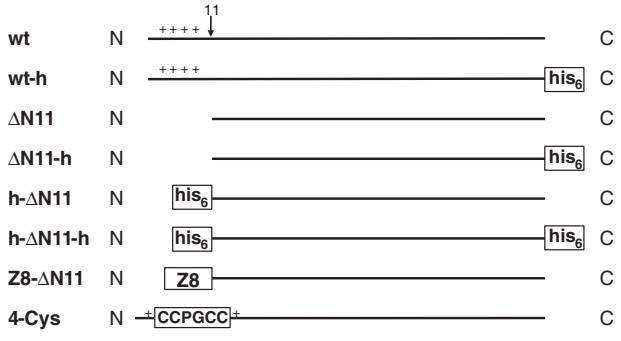

Fig. 1. Schematic sketch of the different LHCII variants used in this work. N and C denote the N and C termini of the proteins. The arrow marked 11 indicates position 11 in the polypeptide chain. The boxed-in segments represent QD-binding affinity tags as explained in the text. The series of "+" designates the N-proximal cluster of positive charges in the wt LHCII protein.

two lutein molecules about 14 chlorophylls, one neoxanthin and substoichiometric amounts of violaxanthin [28].

2.3. Synthesis of water-soluble CdTe/CdSe/ZnS quantum dots

Type-II [29–31] CdTe/CdSe/ZnS quantum dots were synthetized as described elsewhere [23]. The QDs were transferred from toluene into the aqueous phase by ligand exchange reaction with dihydrolipoic acid (DHLA). The concentration of the QDs was taken to correspond to that of the CdTe cores before shell growth, assuming there were no decomposition and no new nucleation of CdTe cores during shell growth. The phase transfer yield was close to 100%.

2.4. Assembly of LHCII and QDs

For titrating LHCII binding to QDs, both components were mixed on ice with tris-(2-carboxyethyl) phosphine (TCEP, 2 mM) and buffer (50 mM sodium-phosphate, pH 8.5, 0.1% (w/v) dodecyl-maltoside, 0.6 M sucrose) to a final volume of 50 μl (centrifugation experiments) or 500 μl (FRET experiments). The QD concentration was kept constant at 0.2 μM (centrifugation experiments) or at 15 nM (FRET experiments) whereas the concentration of the LHCII trimer varied to arrive at molar ratios between 0.5 and 5. The mixtures were incubated for 90 min on ice.

2.5. Ultracentrifugation experiments

Ultracentrifugation experiments have been carried out with a Beckmann Airfuge (rotor: A-110, Beckman Instruments, Munich). The LHCII–QD samples (see Section 2.4) were placed on top of a 130 μl sucrose cushion (1 M sucrose, 50 mM sodium-phosphate, pH 8.5, 0.1% (w/v) dodecyl-maltoside) and centrifuged at 190,000 *g* for 20 min at RT. Then 50 μl of the bottom fraction (with the LHCII–QD pellet) and subsequently 130 μl of the supernatant above the cushion (only LHCII) each were made up to a final volume of 500 μl in the same buffer containing 2 mM TCEP. The samples with the pellet fractions were sonified for 3 min in a bath sonifier (Bandelin, Germany) to suspend the LHCII–QD pellet completely. For determining the LHCII amounts in each sample absorption spectra were recorded.

2.6. Spectroscopic characterization of QDs, LHCII, and hybrid complexes

UV–vis absorption spectra were measured at RT by using an Omega-20 spectrometer (Bruins Instruments) or a V550 UV–vis spectrophotometer (Jasco, Germany). The concentration of LHCII was determined by using an extinction coefficient of $\varepsilon(670\ \text{nm}) = 1{,}638{,}000\ \text{mol}^{-1}\ \text{L}\ \text{cm}^{-1}$ [32].

Photoluminescence (PL) spectra were recorded with a Fluoromax-2 spectrometer (Jobin Yvon, Germany). Spectra were corrected for the wavelength-dependent sensitivity of the fluorometer. The QDs fluorescence quantum yields were estimated by comparing their fluorescence intensity with that of LHCII solutions possessing the same optical density at the excitation wavelength. The LHCII fluorescence quantum yield was determined to be 0.2 as described earlier [28]. For energy transfer calculations, emission spectra of LHCII–QD adducts were fitted by a sum of the individual emission spectra of LHCII and QDs, and the fitted individual spectra were integrated [23].

3. Results and discussion

3.1. Ultracentrifugation experiments are useful for comparing the binding strengths of QD-binding protein tags

For comparing the affinities of different QD-binding protein tags, several LHCII variants (Fig. 1) were generated and mixed with QDs. In this work, type-II CdSe/CdTe/ZnS core–shell QDs coated with

dihydrolipoic acid (DHLA) were used. Wild type LHCII (wt, Fig. 1) binds to QDs via electrostatic interactions between a cluster of positive charges in the protein's N-terminal domain and the negative charges of the DHLA coating on the QD surface. Additionally it has been shown that a C-terminally introduced His_6 tag interacts with Zn^{2+} ions exposed on the QD surface. An LHCII variant lacking the positive charges and containing no additional His_6 tag showed no interaction with the nanoparticles [14,23]. In the present work, two additional QD-binding protein tags were tested and compared to the His_6 tag and the positive-charge cluster. The Z8 peptide sequence, which was described to bind to ZnS surfaces with a relatively high affinity [24] was N-terminally attached to an LHCII version lacking the positive charges in this domain (Z8-ΔN11, Fig. 1). Furthermore, an LHCII version was created with a tetra-cysteine motif (CCPGCC) within the N-terminal domain (4-Cys, Fig. 1). Numerous different ligands have been bound to the ZnS surface of QDs via their sulfhydryl groups [33,34] including the DHLA coating the QDs used in the present work [35].

Relative affinities to QDs of the various binding tags were assessed by a rapid ultracentrifugation assay. Mixtures of 0.3 μM QDs and 0.2 μM LHCII trimers were incubated for 90 min to ensure that the binding equilibrium was reached. In this work LHCII trimers have been used throughout and therefore will be designated as LHCII for simplicity. Measurements of the energy transfer efficiency from LHCII to QDs at room temperature as a function of time revealed that most of the complexes formed within seconds, and after 10–12 min the reaction was completed (data not shown). The QDs with their LHCII ligands bound were then centrifuged at 190,000 *g* through a sucrose cushion and, thus, separated from unbound LHCII, which stayed on top of the sucrose cushion (see Section 2.5). Both the QD pellet and the supernatant were analyzed for their LHCII content by measuring chlorophyll absorption. Assays were evaluated only if at least 80% of the total LHCII amount applied was retrieved. Fig. 2 gives the percentages of the LHCII amounts that were found in the pellet. In the variant ΔN11 the wild type's cluster of positive charges in its N-terminal domain has been deleted (see Fig. 1). Containing no QD affinity tag, ΔN11 was used as a negative control and, as expected, did not appear in the QD pellet. Of the wild type LHCII (wt) 40% was found in the pellet after centrifugation, whereas around 60% of the LHCII variants containing one His_6 tag at the C or at the N terminus (ΔN11-h and h-ΔN11, respectively, see Fig. 1) were bound to QDs, indicating that the His_6-tag mediated binding occurs with higher affinity in comparison to the electrostatic interaction. Both His_6-tagged variants carry the same deletion in the N-terminal domain as described for ΔN11, thus they do not interact with the negatively charged DHLA. This is also true for the LHCII version Z8-ΔN11, which carries the ZnS affinity tag, but only binds at very low amounts (4%) in comparison to the other LHCII variants with binding tags. Of the LHCII variant containing the tetra-cysteine-motif in the N-terminus (4-Cys) 70% was found in the pellet after centrifugation with the QDs. Thus, the affinity of the tetra-cysteine motif to the ZnS surface of the QDs appears to be higher than that of the His_6 tag. In contrast to the LHCII versions listed before, wt-h and h-ΔN11-h (see Fig. 1) contain two binding tags, one at either end of the protein. Wt-h is a derivative of the wild type carrying a His_6-tag at the C-terminus and containing its native N-proximal positive-charge cluster. With 60% found in the pellet this version appears to bind more efficiently compared to wt and with the same affinity as ΔN11-h. If the h-ΔN11-h was used in this centrifugation experiment, 85% of the protein was bound to the QDs. The pellet of these hybrid complexes was difficult to re-solubilize, thus the amount of bound LHCII was calculated from the LHCII found in the supernatant fraction. Both h-ΔN11-h and wt-h in principle are able to crosslink two QDs (see Section 3.3 and Fig. S1 of the supporting information).

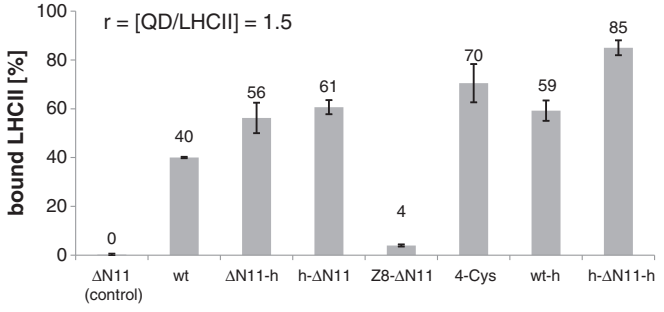

Fig. 2. Binding experiments with QDs and LHCII variants carrying different affinity tags. QDs (0.3 μM) were mixed with LHCII (0.2 μM) and centrifuged through a 1 M sucrose cushion. The amount of QD-bound LHCII in the pellet fraction was assessed by absorption measurements except h-ΔN11-h where the amount of non-bound LHCII in the supernatant was quantitated spectrophotometrically. Error bars indicate standard deviations from three measurements except for wt-h (four measurements) and 4-Cys (10 measurements).

In previous studies gel electrophoresis has been used as a method to separate nanoparticle-bound proteins from unbound proteins [36] as well as for a rough estimation of protein to nanoparticle stoichiometries [37]. Gel electrophoresis allowed us to identify protein binding tags in recombinant LHCII that mediate interaction with semiconductor nanocrystals, i.e. the His_6 tag and a positive charge cluster that interacts with negative charges on the surface of the crystals [14]. However, this technique allowed only a very rough estimate of the binding strengths of these affinity tags whereas the ultracentrifugation experiments presented in this paper detect much slighter differences in affinities (see Fig. 2). The limitation of the gel electrophoresis technique for measuring affinities may be due to the fact that the binding equilibrium is constantly disturbed as the QD–protein complexes migrate through the gel. Ultracentrifugation of the QD–protein complexes through a sucrose cushion is no equilibrium technique either. However, the equilibrium is only disturbed during the presumably very fast passage of the complexes through the cushion. This may explain why the percentage of dissociated complexes detected by ultracentrifugation is larger than expected on the basis of the binding constants measured but still reflects the relative binding strengths of the different protein tags to the QD surface (see further discussion below).

A further benefit of the ultracentrifugation technique in comparison to gel electrophoresis is that the LHCII–QD hybrid complexes are easily accessible in the pellet. After separating the pellet from the supernatant containing the unbound LHCII, the complexes can be suspended and used for further experiments. The extraction of material from a gel is much more difficult and laborious.

3.2. Ultracentrifugation experiments allow estimates of LHCII–QD stoichiometries

For estimating the maximum number of LHCII-trimers that can be bound to the surface of each nanoparticle, QDs at a constant concentration (0.2 μM) were incubated with increasing amounts of LHCII. The LHCII version h-ΔN11 was used, carrying a single affinity tag (see Fig. 1). The LHCII to QD ratios were varied between 0 (no LHCII), 0.5, 1, 2, 4, 6 and 10. The samples were centrifuged through a sucrose cushion and QD-bound and unbound LHCII in the pellet and the supernatant fractions, respectively, was quantitated. When the pellet fraction was removed, some carry-over of material in the supernatant could not be avoided. To take this into account, control experiments were performed for each LHCII concentration in which the QDs were omitted. In these samples there was no pellet, and the amount of LHCII collected after taking out the bottom fraction was taken to be the carry-over and subtracted from the LHCII amount in the pellet fractions of the samples containing QDs. The subtraction amounted to approximately 1% of the applied LHCII.

With increasing LHCII:QD ratios, the amount of LHCII in the pellet increased until it reached saturation between a four- and six-fold excess

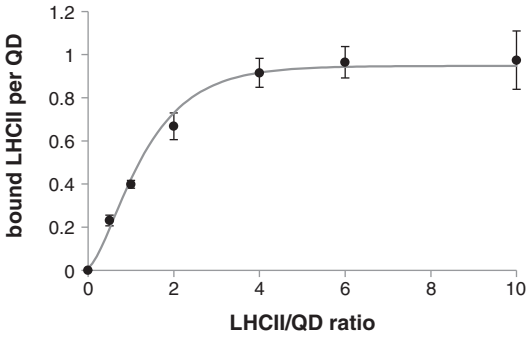

Fig. 3. Estimation of the maximum amount of LHCII trimers (h-ΔN11) bound per QD. A constant concentration of QDs (0.2 μM) was mixed with different concentrations of LHCII-trimers (h-ΔN11) and was centrifuged through a 1 M sucrose cushion. The amount of bound LHCII (pellet fraction) was assessed by absorption measurements. Data have been corrected by the 'carry-over fault' (see text for details). Average (black points) and standard deviation (black bar) are given of three independent measurements. A line to guide the eye only is plotted through the data points.

of LHCII over QDs (Fig. 3). The amount of LHCII bound per QD never exceeded 1 even at a 10-fold excess of LHCII in the mixture.

This result is consistent with our previous study using the same type of LHCII–QD hybrid complexes [23]. In that study the energy transfer from LHCII to QDs indicated that one LHCII per QD bound with high affinity (association constant $K_a \sim 3\ nM^{-1}$). If the excess amount of LHCII over QDs was further increased, the energy transfer rose slightly, indicating that a second LHCII can bind, albeit at a much lower affinity. In the present experiments, the second, low-affinity binding LHCII is likely to dissociate from its QD during their passage through the sucrose cushion.

3.3. FRET assays allow one to assess binding constants of protein–QD hybrid complexes

The type-II QDs used in this work can serve as acceptors of the LHCII excitation energy in a FRET type process. The energy transfer efficiency of this donor–acceptor pair is within a range of 50%, depending on the LHCII version [23]. Consequently, the LHCII donor fluorescence is quenched by approximately 50% in the presence of QDs as an energy acceptor, provided all of the LHCII is QD-bound, for instance by using a saturating amount of QDs. At an equimolar stoichiometry between LHCII and QDs, only a fraction of LHCII is bound to the energy acceptor, consequently only a fraction of the donor fluorescence is quenched in comparison to the maximum quenching in the LHCII–QD complex. This allows one to quantitate unbound and QD-bound LHCII in an equilibrium situation. Examples of the spectral data from which this quantitation was extracted are given in Fig. 4, presenting the 4-Cys (A) and the Z8-ΔN11 (B) protein versions containing a high-affinity and a low-affinity tag, respectively. LHCII binding to QDs was saturated at a 5-fold molar excess of QDs (Fig. 3). Therefore, the LHCII spectra in the absence of QDs (4-Cys and Z8-ΔN11 in Fig. 4) represent the situation with no donor fluorescence quenching and the spectra with a 5-fold excess of QDs [4-Cys + QD (1:5) and Z8-ΔN11 + QD (1:5) in Fig. 4] represent maximum quenching. The strong QD emission peaking at about 750 nm, particularly at the 5-fold excess amount of QD over LHCII, is largely due to the fact that the QDs are co-excited at the LHCII excitation wavelength of 470 nm. However, as documented in our previous publication [23], the quenching of the donor fluorescence is accompanied by an equivalent appearance of sensitized acceptor emission, corroborating the notion that excitation energy transfer takes place as LHCII binds to QD. To correct the LHCII fluorescence emission band from contributions by QD emission in the 1:5 mixtures, the spectra were fitted to linear combinations of the individual emission spectra of LHCII and QDs [23], and the LHCII components of these fits were plotted as 4-Cys fit (1:5) and Z8-ΔN11 fit (1:5) in Fig. 4. Binding at equimolar LHCII–QD stoichiometries was performed at two concentrations, 1.5 nM and 15 nM, examples for the latter being presented in Fig. 4. The comparison of 4-Cys fit (1:1) to 4-Cys and 4-Cys fit (1:5) in Fig. 4A shows about 88% of the maximum quenching at the 1:1 stoichiometry; therefore, 12% of the material stays unbound under this condition. The same comparison for the low-affinity situation in Fig. 4B reveals that in this case 25% of the maximum quenching is observed for a 1:1 stoichiometry, and therefore, 75% of the low-affinity binding LHCII stays unbound.

Because of the equimolarity between QDs and LHCII, the partition of bound vs. unbound material was the same in both cases. With this information we were able to determine binding constants according to the following equation

$$K_a\left[M^{-1}\right] = \frac{[QD * LHCII]}{[QD][LHCII]} \quad (1)$$

with [QD*LHCII] representing the concentration of LHCII–QD complexes, [QD] and [LHCII] representing the concentrations of unbound QDs and LHCII, respectively. The binding constants were calculated from two independent measurements each at 15 nM and 1.5 nM concentrations. The mean values with standard deviations, obtained from the four measurements for each of the differently tagged LHCII–QD hybrid complexes are presented in Table 1.

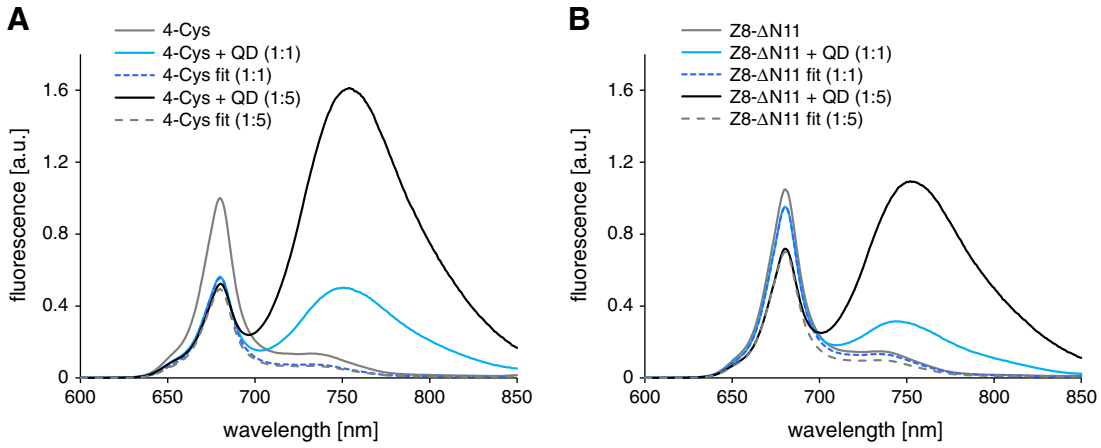

Fig. 4. LHCII variants transfer their energy to CdTe/CdSe/ZnS-DHLA QDs with different efficiencies. A) 4-Cys as example for LHCII with high affinity to QDs. B) Z8-ΔN11 as example for LHCII with low affinity to QDs. Emission spectrum (excitation wavelength: 470 nm) of LHCII (15 nM) with and without QDs (solid gray line). The emission spectra at a 1:1 stoichiometry of LHCII–QD complexes is shown as solid blue line and at a 1:5 ratio as solid black line, the latter representing saturating amounts of QDs. The spectra labeled "fit" (dashed lines) refer to the LHCII components of mixed emission spectra in LHCII–QD mixtures (see text). All samples were measured in the same buffer.

Table 1
The calculated binding constants with standard deviations of different LHCII–QD hybrid complexes from FRET assay experiments. Error margins given represent standard deviation from four independent measurements (two from experiments with LHCII–QD concentrations of 15 nM and two of 1.5 nM).

LHCII variant	K_a [nM^{-1}]
ΔN11	0.00
wt	0.18 ± 0.10
ΔN11-h	0.81 ± 0.21
h-ΔN11	2.22 ± 1.03
4-cys	4.90 ± 1.94
Z8-ΔN11	0.08 ± 0.05

As expected, no FRET was found in the control measurements with ΔN11 and QDs [23]. Without any binding tags the LHCII did not interact with the QDs and thus could not transfer its excitation energy to the QDs. The FRET assays yielded a binding constant of 0.18 ± 0.10 nM^{-1} for wt-QD-hybrid complexes where binding occurs via the protein's N-proximal cluster of positive charges (Table 1). In comparison the K_a values were significantly higher for hybrid complexes with LHCII variants carrying a single His_6 tag, either on the C or the N terminus ($K_{a\ (\Delta N11\text{-}h)} = 0.81 \pm 0.21\ nM^{-1}$; $K_{a\ (h\text{-}\Delta N11)} = 2.22 \pm 1.03\ nM^{-1}$). The slight difference between the affinities of the two His_6 tagged proteins may be explained by the higher flexibility of the N compared to the C terminus [38] facilitating its contact with the QD surface. The binding constants of protein–QD hybrid complexes promoted by a single His_6 tag in the protein sequence are consistent with data in the literature ($K_a \approx 1\ nM^{-1}$) [11].

The LHCII version Z8-ΔN11 with its ZnS-specific affinity sequence was only slightly quenched upon exposure to QDs. Its K_a value ($K_a = 0.08 \pm 0.05$) was even smaller than that of wt. This is unexpected as the Z8 tag has been designed by directed evolution to bind tightly to ZnS surfaces. Presumably, only a small part of the ZnS surface of the QDs is exposed due to the DHLA coating added for water solubility. Possibly the small sections of accessible ZnS surface are not sufficient to serve as an "epitope" of the Z8 affinity peptide. The data obtained here suggest that the Z8 tag, rather than interacting with the ZnS surface of the QDs, binds via its two positive charges (two neighboring arginines) in the Z8 sequence to the negative charges of the DHLA. Wt exhibits a cluster of five positive charges [14] at the N terminus, which may explain that the K_a value of Z8-ΔN11 is smaller compared to that of wt.

The tetra cysteine motif (4-Cys) has the highest affinity to the QDs. The calculated binding constant from FRET-experiments was 4.90 ± 1.94 nM^{-1}. To our knowledge this is the highest binding constant which has been described for hybrid complexes of ZnS coated QDs and proteins.

For the LHCII versions wt-h and h-ΔN11-h the calculation of binding constants is less straight-forward because of the presence of two binding tags. However, as expected, the combination of two His_6 tags (h-ΔN11-h, $K_a = 4.58 \pm 1.84\ nM^{-1}$) or a combination of one His_6 tag and a tag binding electrostatically (wt-h, $K_a = 1.77 \pm 0.52\ nM^{-1}$) resulted in a higher apparent affinity to QDs than a single His_6 tag (ΔN11-h, $K_a = 0.81 \pm 0.21$). The FRET measurements showed that the energy transfer from the LHCII to the QDs under saturation conditions (high excess of QDs) was higher if the LHCII carried two binding tags (h-ΔN11-h with 77% energy transfer or wt-h with 64% energy transfer) compared to the LHCII variant that has only one of these tags (ΔN11-h with 52%, h-ΔN11 with 66% and wt with 41% energy transfer). The ultracentrifugation technique is very useful to assess LHCII–QD stoichiometries at saturating amounts of LHCII (Fig. 3) but not suitable to do the same at an excess amount of QDs since unbound QDs are collected in the pellet together with LHCII–QD complexes.

However, it is highly unlikely that N- and C-terminal His_6 tags in an LHCII trimer can interact simultaneously with one and the same QD. The subunits of an LHCII trimer are oriented in parallel [39,40], thus, all N termini point to one side of the complex and the C termini to the other (see Fig. S1). The C termini are virtually immobile whereas the N terminal domains have some but not unrestricted flexibility [38]. A relatively high mobility has been shown for the first 14 amino acids at the N termini of the wild type LHCII. In case of the LHCII version h-ΔN11-h 11 amino acids in the N terminal domain were replaced by a His_6 tag, leading to a potentially flexible tag of 9 amino acids. If a contour length of 0.38 nm per amino acid is assumed [41], this tag is able to span a maximum distance of 3.4 nm, which clearly is too short to bridge the transmembrane domain of the LHCII with approximately 4.2 nm (see sketch in Fig. S1, data were taken from PDB structure (PDB ID: 2BHW)). For the LHCII version wt-h the simultaneous interaction of N and C termini with the QD surface cannot be rigorously excluded if the non-shortened N-terminal domain is fully stretched out.

In principle, the centrifugation experiments described in Section 3.1 should also be suitable for determining binding constants. However the data of these experiments are not numerically consistent with the binding constants measured by FRET. At the high concentration of reactants used in the centrifugation experiments, the binding is expected to be close to 100%. Interestingly, the amounts of the different LHCII versions co-sedimenting with QDs correlate with the relative binding strengths. A possible explanation is that during sedimentation dissociation kinetics are measured. The lower the binding strength, the faster LHCII dissociates from QDs when the complexes are taken out of their equilibrium during their passage through the sucrose gradient. Consequently, less LHCII is found in the pellet. Therefore, although ultracentrifugation cannot be applied to actually measure binding constants, it commends itself as a rapid technique not only for checking whether a protein (or some other ligand) binds to QDs at all but also for comparing different ligands with regard to their relative binding strengths.

4. Conclusions

In this study, various protein tags were compared with regard to their affinity to core–shell quantum dots with a ZnS surface coated with DHLA. A tetra-cysteine tag (Cys-Cys-Pro-Gly-Cys-Cys) bound significantly more tightly than the often-employed His_6 tag. Binding constants were measured by using energy transfer from QDs to the protein as a monitor for complex formation. Rapid ultracentrifugation through a sucrose cushion was introduced as a new technique for quickly testing whether a protein binds at all to QDs, for assessing binding stoichiometries, and even for comparing binding strengths of different affinity sequences semi-quantitatively. Both techniques can be extended to a vast range of membrane proteins or water-soluble proteins and even to other nanoparticle-binding ligands, provided they are fluorescent, either endogenously or by fluorescent labeling.

Supplementary data to this article can be found online at http://dx.doi.org/10.1016/j.bbagen.2013.11.025.

Acknowledgements

We thank Kristina Gundlach for her contributions in the initial phase of this project and Anita Bohlender for her help with several experiments.

This work has been funded by DFG (SFB 625, TP B7, to T.B. and H.P.) and in its initial part by Stiftung Volkswagenwerk (I/82072, to T.B. and H.P.).

References

[1] W.R. Algar, A.J. Tavares, U.J. Krull, Beyond labels: a review of the application of quantum dots as integrated components of assays, bioprobes, and biosensors utilizing optical transduction, Anal. Chim. Acta. 673 (2010) 1–25.

[2] L. Shao, Y. Gao, F. Yan, Semiconductor quantum dots for biomedical applications, Sensors 11 (2011) 11736–11751.
[3] H. Mattoussi, G. Palui, H.B. Na, Luminescent quantum dots as platforms for probing in vitro and in vivo biological processes, Adv. Drug Deliv. Rev. 64 (2012) 138–166.
[4] W.R. Algar, U.J. Krull, Quantum dots as donors in fluorescence resonance energy transfer for the bioanalysis of nucleic acids, proteins, and other biological molecules, Anal. Bioanal. Chem. 391 (2008) 1609–1618.
[5] A.L. Rogach, Fluorescence energy transfer in hybrid structures of semiconductor nanocrystals, Nano Today 6 (2011) 355–365.
[6] K. Boeneman, J.B. Delehanty, K. Susumu, M.H. Stewart, J.R. Deschamps, I.L. Medintz, Quantum dots and fluorescent protein FRET-based biosensors, Adv. Exp. Med. Biol. 733 (2012) 63–74.
[7] I.L. Medintz, A.R. Clapp, H. Mattoussi, E.R. Goldman, B. Fisher, J.M. Mauro, Self-assembled nanoscale biosensors based on quantum dot FRET donors, Nat. Mater. 2 (2003) 630–638.
[8] K.E. Sapsford, T. Pons, I.L. Medintz, S. Higashiya, F.M. Brunel, P.E. Dawson, H. Mattoussi, Kinetics of metal-affinity driven self-assembly between proteins or peptides and CdSe–ZnS quantum dots, J. Phys. Chem. C 111 (2007) 11528–11538.
[9] A.M. Dennis, G. Bao, Quantum dot–fluorescent protein pairs as novel fluorescence resonance energy transfer probes, Nano Lett. 8 (2008) 1439–1445.
[10] A. Dif, F. Boulmedais, M. Pinot, V. Roullier, M. Baudy-Floc'h, F.M. Coquelle, S. Clarke, P. Neveu, F. Vignaux, R. Le Borgne, M. Dahan, Z. Gueroui, V. Marchi-Artzner, Small and stable peptidic PEGylated quantum dots to target polyhistidine-tagged proteins with controlled stoichiometry, J. Am. Chem. Soc. 131 (2009) 14738–14746.
[11] Y. Zhang, H.Y. Zhang, J. Hollins, M.E. Webb, D.J. Zhou, Small-molecule ligands strongly affect the Forster resonance energy transfer between a quantum dot and a fluorescent protein, Phys. Chem. Chem. Phys. 13 (2011) 19427–19436.
[12] F. Pinaud, D. King, H.P. Moore, S. Weiss, Bioactivation and cell targeting of semiconductor CdSe/ZnS nanocrystals with phytochelatin-related peptides, J. Am. Chem. Soc. 126 (2004) 6115–6123.
[13] H. Mattoussi, J.M. Mauro, E.R. Goldman, G.P. Anderson, V.C. Sundar, F.V. Mikulec, M.G. Bawendi, Self-assembly of CdSe–ZnS quantum dot bioconjugates using an engineered recombinant protein, J. Am. Chem. Soc. 122 (2000) 12142–12150.
[14] W. Erker, S. Boggasch, R.G. Xie, G. Grundmann, H. Paulsen, T. Basché, Assemblies of semiconductor quantum dots and light-harvesting-complex II, J. Lumin. 130 (2010) 1624–1627.
[15] N. Bouchonville, M. Molinari, A. Sukhanova, M. Artemyev, V.A. Oleinikov, M. Troyon, I. Nabiev, Charge-controlled assembling of bacteriorhodopsin and semiconductor quantum dots for fluorescence resonance energy transfer-based nanophotonic applications, Appl. Phys. Lett. 98 (2011) 013703.
[16] S. Pathak, M.C. Davidson, G.A. Silva, Characterization of the functional binding properties of antibody conjugated quantum dots, Nano Lett. 7 (2007) 1839–1845.
[17] E.E. Lees, M.J. Gunzburg, T.L. Nguyen, G.J. Howlett, J. Rothacker, E.C. Nice, A.H. Clayton, P. Mulvaney, Experimental determination of quantum dot size distributions, ligand packing densities, and bioconjugation using analytical ultracentrifugation, Nano Lett. 8 (2008) 2883–2890.
[18] H. Wang, I. Tessmer, D.L. Croteau, D.A. Erie, B. van Houten, Functional characterization and atomic force microscopy of a DNA repair protein conjugated to a quantum dot, Nano Lett. 8 (2008) 1631–1637.
[19] H. Paulsen, B. Finkenzeller, N. Kühlein, Pigments induce folding of light-harvesting chlorophyll *a*/*b*-binding protein, Eur. J. Biochem. 215 (1993) 809–816.
[20] A.R. Cashmore, Structure and expression of a pea nuclear gene encoding a light-harvesting chlorophyll *a*/*b*-binding polypeptide, Proc. Natl. Acad. Sci. U. S. A. 81 (1984) 2960–2964.
[21] K. Kosemund, I. Geiger, H. Paulsen, Insertion of light-harvesting chlorophyll *a*/*b* protein into the thylakoid—topographical studies, Eur. J. Biochem. 267 (2000) 1138–1145.
[22] H. Paulsen, U. Rümler, W. Rüdiger, Reconstitution of pigment-containing complexes from light-harvesting chlorophyll *a*/*b*-binding protein overexpressed in *E. coli*, Planta 181 (1990) 204–211.
[23] M. Werwie, X. Xu, M. Haase, T. Basché, H. Paulsen, Bio serves nano: biological light-harvesting complex as energy donor for semiconductor quantum dots, Langmuir 28 (2012) 5810–5818.
[24] C.E. Flynn, C. Mao, A. Hayhurst, J.L. Williams, G. Georgiou, B. Iverson, A.M. Belcher, Synthesis and organization of nanoscale II–VI semiconductor materials using evolved peptide specificity and viral capsid assembly, J. Mater. Chem. 13 (2003) 2414–2421.
[25] P. Booth, H. Paulsen, Assembly of light-harvesting chlorophyll *a*/*b* complex in vitro. Time-resolved fluorescence measurements, Biochemistry 35 (1996) 5103–5108.
[26] C. Yang, R. Horn, H. Paulsen, The light-harvesting chlorophyll *a*/*b* complex can be reconstituted in vitro from its completely unfolded apoprotein, Biochemistry 42 (2003) 4527–4533.
[27] S. Hobe, S. Prytulla, W. Kühlbrandt, H. Paulsen, Trimerization and crystallization of reconstituted light-harvesting chlorophyll *a*/*b* complex, EMBO J. 13 (1994) 3423–3429.
[28] K. Gundlach, M. Werwie, S. Wiegand, H. Paulsen, Filling the "green gap" of the major light-harvesting chlorophyll *a*/*b* complex by covalent attachment of Rhodamine Red, Biochim. Biophys. Acta Bioenerg. 1787 (2009) 1499–1504.
[29] S. Kim, B. Fisher, H.J. Eisler, M. Bawendi, Type-II quantum dots: CdTe/CdSe(core/shell) and CdSe/ZnTe(core/shell) heterostructures, J. Am. Chem. Soc. 125 (2003) 11466–11467.
[30] R.G. Xie, X.H. Zhong, T. Basché, Synthesis, characterization, and spectroscopy of type-II core/shell semiconductor nanocrystals with ZnTe cores, Adv. Mater. 17 (2005) 2741–2745.
[31] R. Xie, U. Kolb, T. Basché, Design and synthesis of colloidal nanocrystal heterostructures with tetrapod morphology, Small 2 (2006) 1454–1457.
[32] P.J.G. Butler, W. Kühlbrandt, Determination of the aggregate size in detergent solution of the light-harvesting chlorophyll *a*/*b*-protein complex from chloroplast membranes, Proc. Natl. Acad. Sci. U. S. A. 85 (1988) 3797–3801.
[33] I. Yildiz, B. McCaughan, S.F. Cruickshank, J.F. Callan, F.M. Raymo, Biocompatible CdSe–ZnS core–shell quantum dots coated with hydrophilic polythiols, Langmuir 25 (2009) 7090–7096.
[34] N.R. Jana, N. Erathodiyil, J. Jiang, J.Y. Ying, Cysteine-functionalized polyaspartic acid: a polymer for coating and bioconjugation of nanoparticles and quantum dots, Langmuir 26 (2010) 6503–6507.
[35] W.R. Algar, U.J. Krull, Luminescence and stability of aqueous thioalkyl acid capped CdSe/ZnS quantum dots correlated to ligand ionization, ChemPhysChem 8 (2007) 561–568.
[36] L. Li, Q. Mu, B. Zhang, B. Yan, Analytical strategies for detecting nanoparticle–protein interactions, Analyst 135 (2010) 1519.
[37] J. Hou, D.M. Szaflarski, J.D. Simon, Quantifying the association constant and stoichiometry of the complexation between colloidal polyacrylate-coated gold nanoparticles and chymotrypsin, J. Phys. Chem. B 117 (2013) 4587–4593.
[38] C. Dockter, A.H. Muller, C. Dietz, A. Volkov, Y. Polyhach, G. Jeschke, H. Paulsen, Rigid core and flexible terminus structure of solubilized light-harvesting chlorophyll a/b complex (LHCII) measured by EPR, J. Biol. Chem. 287 (2012) 2915–2925.
[39] Z. Liu, H. Yan, K. Wang, T. Kuang, J. Zhang, L. Gul, X. An, W. Chang, Crystal structure of spinach major light-harvesting complex at 2.72 Angstrom resolution, Nature 428 (2004) 287–292.
[40] R. Standfuss, A.C.T. van Scheltinga, M. Lamborghini, W. Kühlbrandt, Mechanisms of photoprotection and nonphotochemical quenching in pea light-harvesting complex at 2.5 Å resolution, EMBO J. 24 (2005) 919–928.
[41] S.R.K. Ainavarapu, J. Brujić, H.H. Huang, A.P. Wiita, H. Lu, L. Li, K.A. Walther, M. Carrion-Vazquez, H. Li, J.M. Fernandez, Contour length and refolding rate of a small protein controlled by engineered disulfide bonds, Biophys. J. 92 (2007) 225–233.